Supported by tetfund
TERTIARY EDUCATION TRUST FUND

STABILIZATION OF MONOVALENT AND MIXED VALENT CATIONS IN SNNOM CLUSTERS AND PREDICTIVE APPLICATIONS – FIRST PRINCIPLES CALCULATIONS

ISSN: 2141 – 3290
www.wojast.org

AHMED A.[A], AUGUSTINE I. A. [A], ANWETING, I.. B.[D].,
SAMSON O. A. [C], PALANICHAMY M.[B]. OLUBUNMI K. A.[A,B*]

[a] Department of Chemistry, Nigerian Army University, P.M.B. 1500, Biu, Borno State, Nigeria.
[b] CSIR-Central Electrochemical Research Institute, Karaikudi-630 006, Tamil Nadu, India.
[c] Federal University of Agriculture, Abeokuta, P.M.B 2240, Abeokuta, Ogun State, Nigeria.
[d] Department of Chemistry, University of Uyo, P. M. B. 1017 Uyo, Akwa Ibom State.
e-mail: olubunmi.kolawole@naub.edu.ng

ABSTRACT

In this work, the stoichiometric dependent structural stability and electronic properties of tin oxide nanoclusters (Sn_nO_m, n = 1 - 6; m = 1 - 2n) is explored by employing first principles density functional calculations. The results show that stable Sn_nO_n ($m = n$) clusters found to have large binding energy, in given n series, due to having high structural symmetry, large energy gap between highest occupied molecular orbital and lowest unoccupied molecular orbital (HOMO-LUMO gap), and univalent charge distributions among Sn and oxygen atoms. On the other hand, stable Sn_nO_{2n} clusters have possessed with mixed charge states of Sn^{2+} and Sn^{4+} ions. The presence of both Sn^{2+} and Sn^{4+} ions in these clusters originates weakly adsorbed O_2 molecule on these clusters, which is quite consistent with earlier experimental work. Interestingly, the structure of some of large sized stable clusters is observed to be resemblance with fused form of two stable isomers. By calculating chemical hardness of Sn_nO_m clusters, we also show that Sn_nO_n clusters are chemically inert and they can be used for optoelectronic devices owing to presence of lone pair Sn^{2+} ions. Whereas, in Sn_nO_m clusters ($m > n$), both Sn^{2+} and Sn^{4+} ions are presented, thus, they can be used for catalytic or sensing applications.

Keywords: Nanoclusters; DFT methods; HOMO-LUMO; Optoelectronic; Catalytic

1.0 INTRODUCTION

Recent years, much attention has been devoted to research on atomic and molecular clusters owing to their interesting size and shape dependent physicochemical properties (Andrievskii and Khachoyan 2010). Hence, they have diverse applications, such as, sensors (Sun *et al.*, 2012), photovoltaic devices (Kumar and Mukherjee 2012), catalysis (Tada *et al.*, 2014), and nanoelectronics (Khan *et al.*, 2019). Besides these applications, the study on deriving the ultra-high stable nanoclusters has been attracted towards fundamental aspects, as they can be considered as building block of various nanostructures (Rahane *et al.*, 2013). Searching the building blocks of compound or bimetallic system is not so simple, as they may not maintain the stoichiometry of respective bulk. The deviation in the stoichiometry of the constituent atoms in compound cluster may be resulted from either the reduction in coordination number of those atoms or possessing mixed valent charge states of atoms presented in the clusters (Simon 1998). In most of cases, the atomic structure of stable compound clusters whose dimensions are in the range of nanometer is quite different from their bulk structure.

In this direction, different stoichiometric early transition metal oxide cations were synthesized by experimental methods for activating C-H bond of methane at room temperature (Zhao *et al.*, 2010). Similarly, Mn-O clusters were produced by laser ablation processing of manganese rod. This study revealed that the prominent species were observed to be $(Mn_nO_m)^{\pm}$ clusters with n/m = ¾. It was also found from density functional theory (DFT) calculations that the excess oxygen atoms are weakly bounded with those stable clusters (Komaya *et al.*, 2015). The size controlled SnO_2 clusters were obtained in mesoporous silica by templating method and their CO oxidation activity is increased with presence of lone pair Sn^{2+} ions (Inomata *et al.*, 2018). Similar context, mixed valence $(Sn_6O_{15})^{-12}$ cluster, having three Sn^{2+} and Sn^{4+} ions each, was synthesized to demonstrate the stereochemically active sites of former ions (Suzuki *et al.*, 2016). Note that the stoichiometry of this cluster is slightly deviated from 1:2 composition. Another study demonstrated that the oxygen rich SnO_2 cluster was found to be more abundant than stoichiometric clusters (Jackson *et al.*, 2002). The stable complex of these nanoparticles with CO species was also explained by DFT calculations, to demonstrate the stability of those clusters towards to catalytic activity (Mazzone and Morandi 2007). On the other hand, these clusters can be used as hydrogen and ammonia sensors (Boyd and Brown 2009). Among the post transition oxides, SnO_2 is cheaply available and also, is well attracted due to versatile technological applications (Gaggiotti *et al.*, 1994; Idota *et al.*, 1997; Nehru *et al.*, 2012; Pedersen and Luisier 2014; Larin *et al.*, 2016; Yu *et al.*, 2016; Barbe *et al.*, 2017; Wali *et al.*, 2018; Manjunathan *et al.*, 2018) Though, there are lot of experimental works on SnO_2 clusters and few theoretical works (Liu *et al.*, 2003; Nehru *et al.*, 2012; Li *et al.*, 2016) had been attempted. However, the stoichiometry dependent clusters have not been studied well. Hence, we studied Sn-O nanoclusters by employing DFT calculations to unveil the structural and electronic properties of various Sn_nO_m nanoclusters ($n = 1 – 6$ and $m = 1 – 2n$) to understand their stoichiometric dependency of valent distribution and physicochemical properties of the Sn_nO_m nanoclusters. The origin of preference of the mixed valence charge states of Sn in SnO_2 clusters ions are discussed in this work.

2.0 COMPUTATIONAL METHODOLOGY

All results presented in this work are carried out using plane wave based first principles DFT calculations as implemented in Vienna *Ab initio* Simulation Package (VASP) (Kresse and Furthmuller 1996). Sn and O atoms are described by projector augmented wave pseudopotential formalism (PAW) (Blöchl 1994) and exchange correlations for electron-electron interactions are corrected by generalized gradient approximations (GGA) (Perdew *et al.*, 1996). The kinetic energy cut-off of 500 eV is used for plane-wave basis sets. The valence electronic configuration of Sn and O atoms are described by $5s^25p^2$ and $2s^22p^4$, respectively. The clusters are kept in large cubic cell which maintain the separation between the cluster and its periodic images, at least 8.5 Å and this separation is to avoid the interaction between them. The Brillouin zone is sampled using Gamma point. All the ions are completely relaxed without considering the symmetry. The iterative relation process is repeated until the absolute force on each ion is converged to order of 0.01 eV/Å and the energy difference between two ionic steps is converged to 10^{-5} eV in all the calculations. After performing non-spin polarised calculations, the spin polarized calculations are also employed to determine the possibility of magnetism in the clusters.

3.0 RESULTS AND DISCUSSION

3.1 Structural and electronic properties of Sn_n

To understand the stoichiometry dependent structural stability and electronic properties of Sn_nO_m clusters, we initially considered Sn_n clusters ($n = 1 - 6$). The stable Sn_n isomers are deduced by employing first principles calculations and the optimized structures are shown in Fig. 1. The geometries of stable Sn_n isomers with $n = 1 - 6$ are dot, linear, V-bent, rhombus, triangular bipyramid, and octahedron, respectively. It is also noted that those geometries are well matched with reported literature (Behnam *et al.*, 2009), which reveals the consistency of our calculations. Next, we show the binding energy (BE) and electronic properties of stable Sn_n clusters along with their structural properties as shown in Table 1. It deduced that BE and the energy gap between highest occupied molecular orbital (HOMO) and lowest unoccupied molecule orbital (LUMO) increases with size of the cluster. It is interested to observe that only Sn dimer prefers to stabilize with the magnetic moment of 2 μ_B when compared to non-magnetic isomer as two electrons lied closer to HOMO level are occupied in doubly degenerated π - orbitals. In addition to that, for Sn_3 cluster, V-bent isomer is more stable while equilateral triangular isomer is not forming due to present of lone pair Sn^{2+} ions.

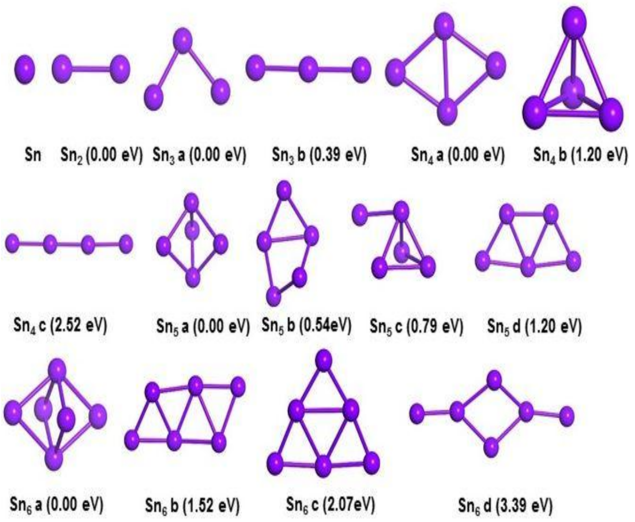

Fig. 1: Optimized structures of Sn_n ($n = 1 - 6$) clusters are considered for this work. Various isomers (indexed with *a*, *b*, *c*, *d*) are given and their energies with respect to stable isomer are provided in bracket.

Table 1: BE and HOMO-LUMO gap of stable Sn_n clusters ($n = 1 - 6$) are given along with their magnetic moment, Sn-Sn bond distance, and bond angle.

n	BE (eV/atom)	HOMO-LUMO gap (eV)	M (μ_B)	Bond distance (Å)	Bond angle (deg)
2	1.37	0.31	2	2.8	
3	1.94	0.82	-	2.7	79.8
4	2.38	1.04	-	2.86 – 3.02	64 – 116
5	2.56	1.56	-	2.8	80 – 83
6	2.74	1.6	-	2.9	70 – 109

3.2 Structural and electronic properties of Sn_nO_m

In order to deduce various isomers for Sn_nO_m ($n = 1 - 6$, $m = 1 – 2n$) clusters, oxygen atoms are systematically decorated into stable and low lying isomers of Sn_n clusters. It is worthy to mention that we have considered nearly 250 clusters for this work. All optimized isomers along with the energetics, with respective to stable isomers, are reported (see supporting information Fig. S1). The BE of those clusters, as similar to pure tin cluster, are deduced from

$$BE = \frac{nE(Sn)^q + mE(O) - E(Sn_nO_m)^q}{m+n}$$

where $E(Sn)^q$, $E(O)$, and $E(Sn_nO_m)^q$ are atomic energy of Sn, O, and total energy of $Sn_nO_m{}^q$ nanoclusters respectively and q is the electronic charge of clusters (-1, 0, and +1).

The calculations on charged clusters are carried out to deduce the physiochemical properties as discussed in the later section. The bond distances, charge states of Sn atoms, BE, and HOMO-LUMO gap of stable Sn_nO_m clusters are shown in supporting information Table S1 and their optimized structures are presented in Fig. S2. It indicated that in the stable Sn_1O_1 and Sn_1O_2 clusters, Sn atom is terminated with, respectively, one and two oxygen atoms with the bond distance of 1.8 Å. On the other hand, the oxygen atoms prefer to bind with Sn_2 through edge fashion (Sn-O bond distance = 2.05 Å), until edge sites are occupied. After occupying all those sites, the oxygen atoms opt to place the terminal sites of the cluster. The reason for occupation of oxygen atoms in this kind is that the stable geometries of Sn_2O_m clusters (m = 1 - 4) favoured to maximize the Sn-O bond without much affecting the Sn-Sn bond, as the strength of former bond is 3.37 eV (at equilibrium distance of 1.8 Å), which is quite high as compared to Sn-Sn bond strength (1.37 eV, at 2.8 Å). This trend is also continued in Sn_3O_m clusters. In this case, the priority of occupation of oxygen atoms is face, edge, and terminal sites. Even though, the occupation of oxygen atoms at facial sites maximizes more number of Sn-O bonds in the cluster, but the bond distances are varied from 2.1 to 2.4 Å, due to having the limited directional character of *s* and *p* orbitals that are involved in the bonding of those clusters. This effect can be visualized in stabilizing the Sn_3O_3 cluster, where three oxygen atoms prefer to occupy at edge positions, rather than facial sites of Sn_3 triangle. Moreover, stable isomer of Sn_3O_3 cluster is having the high symmetry as compared to other isomers (refer Fig. S1, Supporting Information). This kind of structure was also reported to be stable in CdS nanoclusters (Karthikeyan *et al.*, 2012). The mixture of oxygen atoms occupying at edge, face, and/or terminal sites of Sn_3 cluster is found to be observed in stable isomers of Sn_3O_4 and Sn_3O_5. It is also understood that the stability of those isomers is arisen owing to having the high structural symmetry, sufficient separation between oxygen atoms to nullify their repulsive interactions, and maximizing Sn-O bonds without losing Sn-Sn bonds. It is interesting to observe the stable isomer for Sn_3O_6 cluster (refer Fig. 2), in which, O_2 molecule (bond distance = 1.31 Å) is weakly bonded with Sn_3O_4 isomer. Adsorption energy of the oxygen to a stable cluster is calculated from

$$E_{ads} = E(Sn_nO_m) - E\left(Sn_nO_{(2n-2)}\right) - E(O_2)$$

where $E(Sn_nO_m)$ is the total energy of Sn_nO_m clusters, and $E(O_2)$ is the total energy of O_2 molecule.

The calculated adsorption energy of O_2 molecule onto Sn_3O_4 cluster is -0.25 eV. This adsorption energy is not sufficient to quench the magnetism in O_2 molecule as we observed the spin moment of 2 μ_B in this nanocluster. Due to having weak adsorption energy and maintaining the magnetism in the molecule, Sn_3O_4 cluster can be potentially used for sensing of oxygen molecule.

Our work extended on deducing the stable isomers for Sn_4O_m, Sn_5O_m, and Sn_6O_m clusters and the optimized structures are given in Fig. 2. Overall, geometries with oxygen atoms decorated on Sn closed structure are found to be stable until little higher stoichiometry ratio of 1:1. As example, the closed geometry is observed to be stable for Sn_4O_m (m = 1 – 5), Sn_5O_m (m = 1 – 6), and Sn_6O_m (m = 1 – 8) clusters. Beyond this stoichiometry limit, open structures, such as, Sn_4 rhombus, Sn_5 trapezoid, and Sn_6 parallelogram, are observed to be stable as these structures can accommodate more number of oxygen atoms.

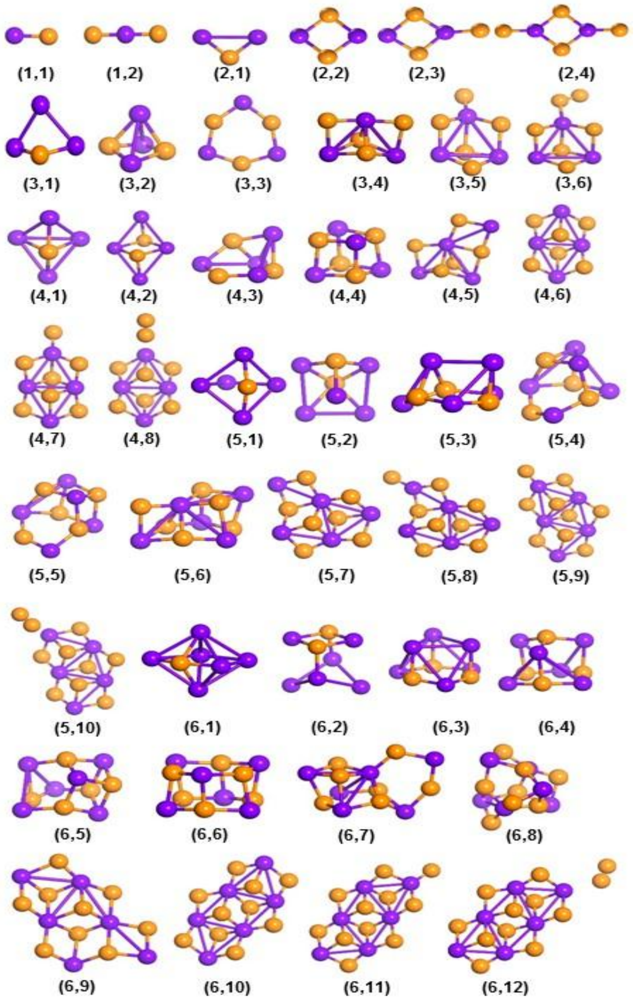

Fig. 2: Stable isomers of Sn_nO_m (n = 1 - 6, m = 1 – 2n) clusters. (n, m) values are given in each cluster. Purple and golden yellow balls represent Sn and O atoms, respectively.

As discussed earlier, priority of occupation of oxygen atoms in Sn cluster is in order of face/edge sites and terminal sites. After occupying all face or edge sites by oxygen atoms, terminal site is preferred. For example, one additional oxygen atom introduced into the stable isomers of Sn_4O_6 and Sn_6O_{10} is intended to occupy one of their terminal sites. When two oxygen atoms added into these isomers, they are preferred to attach as O_2 molecule, rather than occupying as two terminal sites (refer Fig. 4). We also calculated the adsorption energy of oxygen molecule on those isomers and it is found to be >0.1 eV, indicating that the molecule is weakly adsorbed on cluster. Thus, these clusters can be potentially used for sensing of oxygen molecule.

To understand the stoichiometry dependent structural stability and electronic properties of Sn_nO_m clusters, the BE and HOMO-LUMO gap are reported in Fig. 3 and Table S1 (Supporting Information). The BE value increases with m until 1:1 stoichiometry, then it is decreased, gradually, due to accommodating more of oxygen atoms. Based on the energetics, the compound cluster with 1:1 stoichiometry prefers to stabilize easier than other stoichiometric clusters. Similarly, the HOMO-LUMO gap of the clusters with $n = m$ has higher value when compared to clusters with $n \neq m$. It is also observed that the cluster with $m = 2n$ has relatively large gap and also, those values do not deviate much from Sn_nO_{2n-2} clusters. Due to the effect of lone pair- lone pair repulsion between the Sn (II) ions, there is large bond distance of Sn-Sn bond in some of the nanoclusters. This can be explained as a result of strong interaction between Sn(5*s*) and O(2*p*) which is resulted to strong lone pair repulsion (Walsh and Watson 2005; Payne *et al.*, 2006).

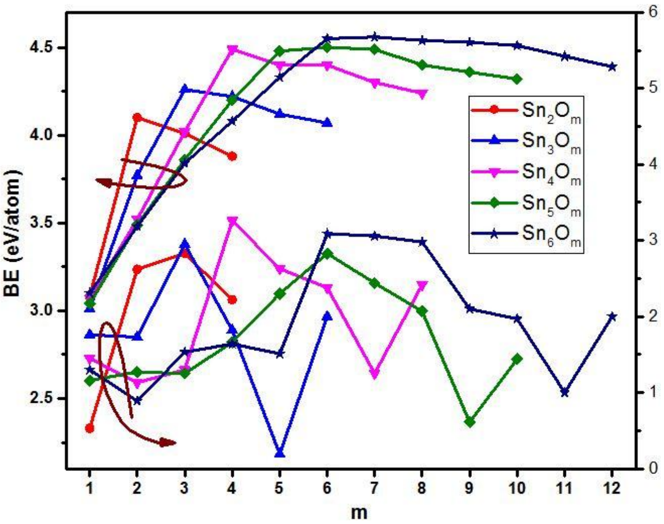

Fig. 3: BE and HOMO-LUMO gap of stable Sn_nO_m clusters are shown.

The Bader charge analysis was carried out to understand the charge state of atoms presented in the clusters while the charge state of Sn atoms are reported in Table S1 (Supporting Information). It shows that Sn atoms in all stable clusters prefer to be Sn^{2+} and/or Sn^{4+} charge states, rather than Sn^{3+} state. Note that in few cases, Sn atom is found to be +1 state. It is also obvious that Sn_nO_n cluster has only Sn^{2+} state, owing to uniform charge distribution between Sn and O atoms presented in the clusters, while Sn_nO_{2n} clusters has both Sn^{2+} and Sn^{4+} ions due to the existence of neutral oxygen molecule. On the other hand, oxygen atoms that are bonded with Sn cluster get two electrons from Sn atoms, whereas the oxygen molecule formed in stable Sn_nO_{2n} clusters ($n > 2$) prefers to be in neutral charge state. We also observed that the molecules with charge state of O_2^- and O_2^{2-} (including O^{2-} ion formed cluster) are also stabilized in less stable clusters (refer Fig. 4). Due to taking the charge from Sn atom, Sn-Sn bond distance is decreased to 3.14 Å, as varying charge state from Sn^{2+} to Sn^{4+}. Thus we concluded that monovalent Sn^{2+} ions are presented in Sn_nO_n clusters, while mixed valence Sn ions are possessed in stable Sn_nO_m ($m > n$) clusters.

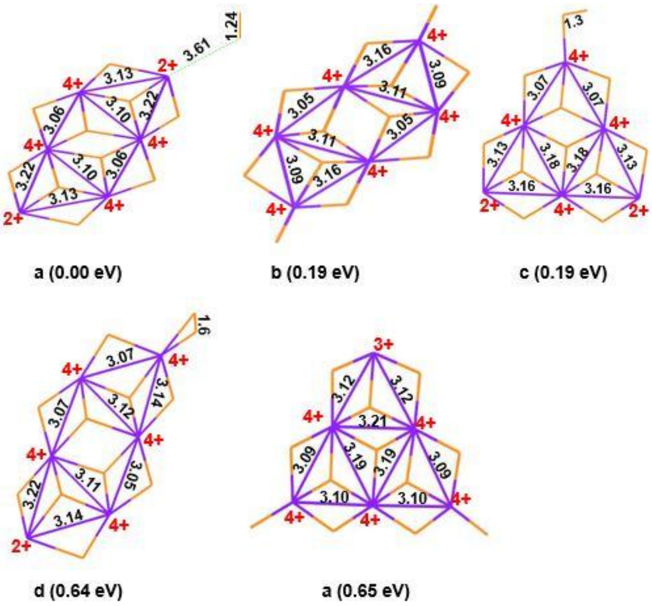

a (0.00 eV) b (0.19 eV) c (0.19 eV)

d (0.64 eV) a (0.65 eV)

Fig. 4: Representative cases of various Sn_6O_{12} isomers (stick model) are shown. The energy values are given with respect to stable isomer. The charge state of Sn atoms and Sn-Sn, Sn-O, and O-O bond distances (in Å) are also indicated.

3.3 Fragmentation energy (FE) of Sn_nO_m clusters

We observed that the geometry of some stable clusters are observed to be fused units of two small clusters (refer Fig. 1). As example, two units of Sn_2O_2 and Sn_3O_3 clusters are condensed to form Sn_4O_4 and Sn_6O_6 clusters, respectively. Similarly, the geometry of Sn_5O_3 cluster is deduced by fusing of Sn_2 and Sn_3O_3 clusters. With this intuition, we calculated the fragmentation energy of various clusters which are reported in Table 2 along with fused units. The fragmentation energy is calculated from

$$FE = -E(Sn_nO_m) + E\left(Sn_{(n-x)}O_{(m-y)}\right) + E\left(Sn_xO_y\right)$$

where $E(Sn_nO_m)$ is the total energy of the fused cluster and $E\left(Sn_{(n-x)}O_{(m-y)}\right)$ and $E\left(Sn_xO_y\right)$ are the total energy of the respective fragments. It shows that the oxygen molecule is weakly adsorbed in most of stable clusters, whose stoichiometry is closer to 1:2. Whereas, Sn_6O_8 cluster will liberate the oxygen molecule by applying the energy of 2.14 eV. Oxygen molecule is easily liberated from stoichiometric

SnO_2 clusters that is resulted to stabilize the Sn_nO_{2n-2} cluster, which also, has relatively large HOMO-LUMO gap as compared to other Sn_nO_m clusters. On the other hand, two Sn_nO_n units are strongly bonded to form condensed clusters, which can be potentially formed into SnO nanowire as discussed in Sn-Se (Nagarajan and Chandiramouli 2014) and Cd-S (Karthikeyan *et al.*, 2012) nanowires.

Table 2: Fragmentation energy (FE) of Sn_nO_m clusters are given with fragments involved in process.

Clusters	**FE (eV)**
Sn_2O_2 (SnO, SnO)	2.91
Sn_3O_4 (SnO_2, Sn_2O_2)	2.93
Sn_3O_5 (SnO_3,Sn_2O_2)	2.81
Sn_3O_6 (Sn_3O_4, O_2)	0.25
Sn_4O_2 (Sn_2O, Sn_2O)	2.65
Sn_4O_4 (Sn_2O_2, Sn_2O_2)	3.12
Sn_4O_8 (Sn_4O_6, O_2)	0.03
Sn_5O_3 (Sn_2, Sn_3O_3)	2.60
Sn_5O_4 (Sn_2O, Sn_3O_3)	3.01
Sn_5O_5 (Sn_2O_2, Sn_3O_3)	2.82
Sn_5O_7 (SnO, Sn_4O_6)	3.19
Sn_5O_{10} (Sn_5O_8, O_2)	0.03
Sn_6O_2 (Sn_4, Sn_2O_2)	1.90
Sn_6O_3(Sn_3, Sn_3O_3)	3.21
Sn_6O_4(Sn_3O_2, Sn_3O_2)	3.14
Sn_6O_4 (Sn_3O, Sn_3O_3)	3.15
Sn_6O_6(Sn_3O_3, Sn_3O_3)	3.46
Sn_6O_8(Sn_6O_6, O_2)	2.14
Sn_6O_{11}(Sn_6O_9, O_2)	0.86
Sn_6O_{12}(Sn_6O_{10}, O_2)	-0.14

3.4 Electronic properties of Sn_nO_m nanoclusters

We carried out the calculations on the structural stability and electronic properties of charged (both cationic and anionic) Sn_nO_m nanoclusters in reference to reported method (Xu *et al.*, 2014). The BE and HOMO-LUMO gap of charged clusters are deduced and values are compared with that of neutral clusters (Fig. 5 and Fig. S2, Supporting Information). It shows that the BE of cationic clusters is always higher than respective neutral and anionic clusters. This reveals that Sn_nO_m cluster prefers to be stabilized in cationic form. To support this statement, the HOMO-LUMO gap of cationic clusters is higher than that of anionic clusters. The trend of gap versus *m* values of former clusters is well matched with neutral clusters. Thus, neutral Sn_nO_m clusters donate one electron without much effect in HOMO-LUMO gap, as Sn atoms retain a few electrons on them after transferring most of electrons to oxygen atoms.

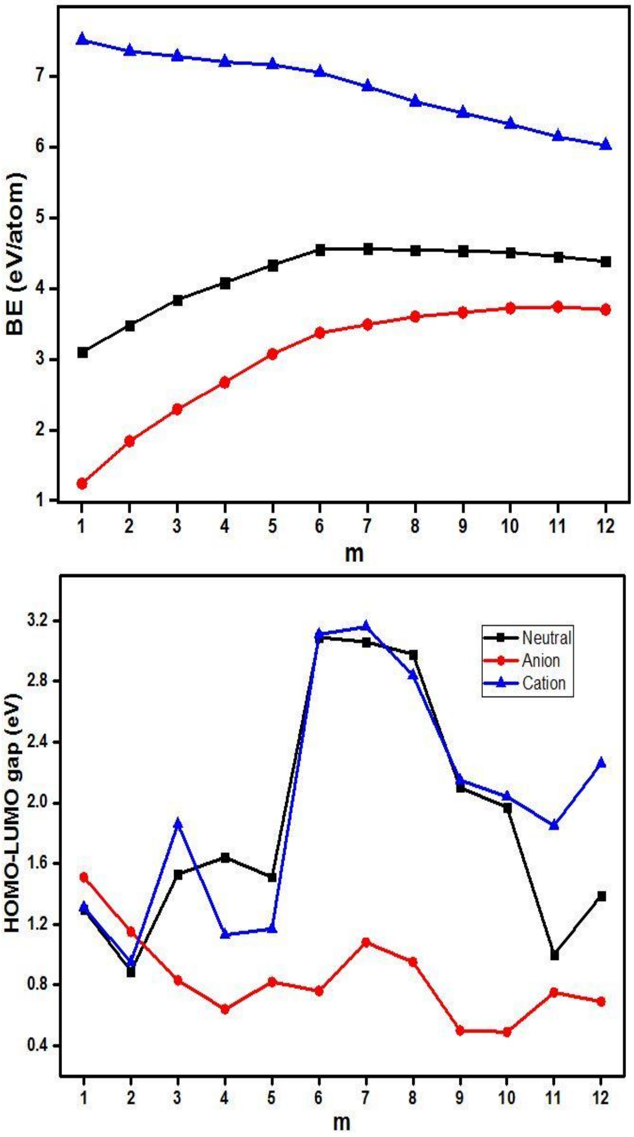

Fig. 5: (a) BE and (b) HOMO-LUMO gap of cationic, anionic, and neutral Sn_6O_m clusters are shown for various *m* values.

3.5 Physicochemical properties of Sn_nO_m nanoclusters

Finally, we have also calculated the vertical ionization potential (IP), electron affinity (EA), chemical potential (μ), and chemical hardness (η) of stable Sn_nO_m clusters to understand their physio-chemical properties from following formulae

$$IP = E(cation) - E(neutral) \quad \dots\dots\dots\dots\dots\dots\dots\dots. (1)$$

$$EA = E(neutral) - E(anion) \quad \dots\dots\dots\dots\dots\dots\dots\dots. (2)$$

$$\mu = \frac{IP+EA}{2} \quad \dots\dots\dots\dots\dots\dots\dots\dots\dots\dots\dots\dots\dots\dots\dots. (3)$$

$$\eta = \frac{IP-EA}{2} \quad \dots\dots\dots\dots\dots\dots\dots\dots\dots\dots\dots\dots\dots\dots\dots (4)$$

The deduced values are given in Table S1 (Supporting Information). It shows that IP value is strongly dependent on oxygen content in the clusters (beyond $n > 2$). The IP values increases with increase in oxygen content due to reduction in the metallic character of the clusters. It is also observed that Sn_nO_n and Sn_nO_{2n-2} clusters have significant increment in IP values as compared to nearby stoichiometric clusters, which confirms their higher structural stability. This scenario is reflected in EA, chemical potential, and chemical hardness. It is interested to notice that the chemical hardness of Sn_nO_m ($n = m$) cluster is always higher than that of clusters with $m = 2n$. It indicates that former type of clusters can be used for fabricating optoelectronic devices as they have only presented the stereochemically active Sn^{2+} ions. Even though Sn^{2+} ions are having metastable character, they can be stable as a cluster owing to interaction among the ions. On the other hand, both Sn^{2+} and Sn^{4+} ions are presented in $Sn_{\underline{n}}O_m$ clusters ($m > n$), therefore, they can be used for catalytic or sensing applications.

4.0 CONCLUSION

In the present work, we have investigated the structural stability of Sn_n and Sn_nO_m nanoclusters by modelling different structural isomers to understand the valent variation and stoichiometric dependency of physiochemical properties of the clusters. The calculated BE revealed that stable Sn-O clusters with 1:1 stoichiometry have higher energy as compared to other stoichiometric clusters owing to their high symmetry, large HOMO-LUMO gap, and univalent charge distribution among Sn and O atoms. This effect is also reflected in HOMO-LUMO gap and other chemical properties. We also performed the spin polarization calculations on each clusters and results indicated that Sn_3O_6, Sn_4O_8, Sn_5O_{10} and Sn_6O_{12} (1:2) have magnetic properties, owing to weakly adsorbed magnetic O_2 molecules. Mixed valent Sn ions are presented in stable Sn_nO_{2n} clusters due to O_2 molecule weakly adsorbed on those clusters. The structure of some of stable isomers is quite similar to fused form of two small clusters. Calculations on chemical hardness of Sn_nO_m clusters shows that SnO clusters are chemically inert and they can be used for optoelectronic electronic devices due to the presence of Sn^{2+} ions, while the presence of both Sn^{2+} and Sn^{4+} ions in $Sn_{\underline{n}}O_m$ clusters ($m > n$) can be used for catalytic or sensing applications.

Supporting Information Available:

1) BE and HOMO-LUMO gap of stable Sn_n clusters, 2) Various isomers are considered for identifying stable isomers of Sn_nO_m clusters, 3) BE and HOMO-LUMO gaps of neutral, cationic and anionic Sn_nO_m clusters, 4) Physicochemical properties of $Sn_6\,O_m$ clusters.

Acknowledgements

Authors the World Academy of Science and Council of Scientific and Industrial Research (CSIR-TWAS) for the opportunity of research fellowship granted to him. Authors also thank CSIR-Central Electrochemical Research Institute, Karaikudi, Tamil Nadu, India for the provision of facilities to carry out the research.

Conflicts of interest

Authors declare that there are no conflicts of interest.

5.0 REFERENCES

Andrievskii, R.A. and Khachoyan, A.V. (2010). Role of size-dependent effects and interfaces in physicochemical properties of consolidated nanomaterials. *Russian Journal of General Chemistry*, **80**: 555-566.

Barbe, J., Tietze, M.L., Neophytou, M., Murali, B., Alarousu, E., Labban, A.E., Abulikemi, M., Yue, W., Mohammed, O.F., McCulloch, I., Amassian, A. and Gobbo, S.D. (2017). Amorphous Tin oxide as a low-Temperature-Processed electron-Transport layer for organic and hybrid perovskite solar cells. *ACS Applied Materials and Interfaces*, 9: 11828-11836.

Behnam A., Sascha S., Peter S. (2009). Electronic properties for small tin clusters Sn_n ($n \leq 20$) from Density Functional Theory and the convergence toward the solid state. *Journal of Computational Chemistry*, 31(5): 929-937.

Blochl P.E. (1994), Projector augmented-wave method. *Journal of Physical Review*, 50(24): 17953- 17979.

Boyd, E.J. and Brown, S.A. (2009). The size dependence of tin oxide atomic cluster nanowire field effect transistors. *Nanotechnology*, 20: 425201, 1 – 7.

Gaggiotti G.; Galdikas A.; Kačiulis S.; Mattogno G.; Setkus A. (1994). Surface chemistry of tin oxide based gas sensors. *Journal of Applied Physics*, 76(8): 4467 – 4471.

Idota, Y., Kubota, T., Matsufuji, A., Maekawa, Y., and Miyasaka, T. (1997). Tin-Based Amorphous oxide: A high-capacity Lithium-ion-storage material. *Science*, 276: 1395-1397.

Inomata, Y., Albrecht, K., and Yamamoto, K., (2018). Size-dependent oxidation state and CO oxidation activity of Tin oxide clusters. *ACS catalysis*, 8: 451-456.

Jackson, P., Fisher, K.J., Dance, I.G., Gadd, G.E. and Willet, G.D., (2002). The Structure of Gas Phase Tin Oxide Ions Generated by Laser Ablation: A Combined Fourier Transform Mass Spectrometry and Density Functional Theory Study, *Journal of Cluster Science*, 13(2): 165 – 187.

Karthikeyan S., Deepika E. and Murugan P. (2012). Structural Stability and Electronic Properties of CdS Condensed Clusters. *Journal of Physical Chemistry C*, 116: 5981-5985.

Khan. I., Saeed, K., Khan, I., (2019). Nanoparticles: Properties, applications and toxicities *Arabian Journal of Chemistry*, 12(7): 908 - 931.

Koyama, K., Kudoh, S., Miyajima, K. and Mafune, F. (2015). Stable stoichiometry of Gas-Phase manganese oxide cluster ions revealed by temperature-programmed desorption. *Journal of Physical Chemistry A*, 119: 8433-8442.

Kresse G.; Furthmuller J. (1996). Efficient iterative schemes for *ab initio* total-energy calculations using a plane-wave basis set. *Journal of Physical Review*, 54(16): 11170 - 11185.

Kumar, S. and Mukherjee, C. (2012). Role of Plasmons in Improved Photovoltaic Devices: Nanoclusters of Sn and SnO_x in SnO_2 films. *International Conference on recent trend in Physics Journal of Physics*,365 (012008): 1-7.

Larin, A., Womble, P.C., Dobrokhotov, V. (2016). Hybrid SnO_2/TiO_2 nanocomposites for selective detection of ultra-low Hydrogen sulfide concentrations in complex backgrounds. *Sensors*, 16(1373): 1-15.

Li, Y., Singh, D.J., Du, M.-H., Xu, Q., Zhang, L., Zheng, W. and Ma, Y. (2016). Design of ternary alkaline-earth metal Sn (II) oxides with potential good p-type conductivity. *Journal of Materials Chemistry C*, 4**:** 4592-4599.

Liu, Z., Zhang, D., Han, S., Li, C., Tang, T., Jin, W., Liu, X., Lei, B. and Zhou, C. (2003). Laser ablation synthesis and electron transport studies of tin oxide nanowires. Advanced Materials, 15(20): 1754-1757.

Manjunathan, P., Marakatti, V.S., Chandra, P., Kulal, A.B., Umbarkar, S.B., Ravishankar, R., Shanbhag, G.V. (2018). Mesoporous tin oxide: An efficient catalyst with versatile applications in acid and oxidation catalysis, *Catalysis Today*, 309: 61 – 76.

Mazzone, A.M. and Morandi, V. (2007). CO adsorption onto tin oxide clusters: DFT calculations. *Computational Materials Science*, 38: 814–823.

Nagarajan V. and Chandiramouli, R. (2014). Exploring structural stability and electronic properties of SnSe nanostructures-A DFT study. *Der Pharma Chemica*, 6(2): 239-251.

Nehru L.C.; Swaminathan V.; Sanjeeviraja C. Photoluminescence studies on nanocrystalline tin oxide powder for optoelectronic devices. *American Journal of materials Science*, 2(2): 6-10.

Payne D.J., Egdell, R.G., Walsh, A., Watson, G.W., Guo, J., Glans, P.A., Learmonth, T., Smith, K.E. (2006). Electronic Origins of Structural Distortions in Post-Transition Metal Oxides: Experimental and Theoretical Evidence for a Revision of the Lone Pair Model. *Physical Review Letters*, 96: 1-4.

Pedersen, A. and Luisier, M. (2014). Lithiation of Tin Oxide: A Computational study. *ACS Applied Materials Interfaces*, 6: 22257-22263.

Perdew, J.P., Burke, K. and Ernzerhof, M. (1996). Generalized Gradient Approximation Made Simple. *ACS Physical Review letter*, 77(18): 3865-3868.

Rahane, A.B., Murkute, P.A., Deshpande, M.D. and Kumar, V. (2013). Density Functional calculations of the structural and electronic properties of $(Y_2O_3)_n^{0,\pm1}$ clusters with n = 1-10. *Journal of Physical Chemistry A*, 117: 5542-5550.

Simon, A. (1988). Clusters of Valence Electron Poor metals-Structure, Bonding and Properties. *Angewandte Chemica International Edition English*, 27: 159-183.

Sun, Y.F., Liu, S.-B., Meng, F.L., Liu, J.Y., Jin, Z. (2012). Metal Oxide Nanostructures and their gas sensing properties: A review. *Sensors*, 12: 2610-2631.

Suzuki, K., Hanaya, T., Sato, R., Minato, T., Yamaguchi, K., and Mizuno, N. (2016). Hexanuclear Tin (II) and mixed valence Tin (II,IV) oxide clusters within polyoxometalates. *Chemical Communi*cation, 52: 10688-10691.

Tada, H., Jin, Q., Iwaszuk, A., Nolan, M. (2014). Molecular-scale transition metal oxide nanocluster surface-modified titanium dioxide as solar-activated environmental catalysts. *Journal of Physical Chemistry C*, 118: 12077-12086.

Wali, Q., Iqbal, Y., Pal, B., Lowe, A., Jose, R. (2018). Tin oxide as an emerging electron transport medium in perovskite solar cells. *Solar energy materials and Solar cells*, 179: 102-117.

Walsh, A. and Watson, G.W. (2005). Influence of the Anion on Lone Pair Formation in Sn (II) Monochalcogenides: A DFT Study. *Journal of Physical Chemistry B*, 109: 18868-18875.

Xu, L., Xia, C.-J., Wang, L.-F., Xie, L., Wang, B., Zang, Y.-F., Huang, X. (2014). Structural evolution, sequential oxidation and chemical bonding in tri-yttrium oxide clusters: $Y_3O_x^-$ and Y_3O_x (x = 0-6) RSC Adv. 2014, 4, 60270-60279.

Yu, X., Marks, T.J., Facehetti, A. (2016). Metal oxides for optoelectronic applications. *Nature materials*, 15, 383-396.

Zhao, Y. -X., Wu, X.-N., Wang, Z.-C., He, S.-G. and Ding, X.-L. (2010). Hydrogen-atom abstraction from methane by stoichiometric early transition metal oxide cluster cations. *Chemical Communication*, 46: 1736-1738.